



ANTI-PROLIFERATIVE PROPERTIES OF THYMOQUINONE TO OVERCOME CISPLATIN-INDUCED DRUG RESISTANCE IN SKOV-3

Shivani S. Tendulkar¹, Aishwarya Hattiholi², Vijay Kumbar³, Meenaz Sangolli⁴,
Mehul A. Shah⁵, Kishore Bhat⁶, Suneel Dodamani^{7*}

Abstract

Background: Ovarian cancer (OvCa) malignancy is a widespread type of cancer with a poor prognosis contributed by resistance developed against platinum-based drugs. The use of phytochemicals has been an innovative key for the treatment of OvCa. The antiproliferative properties of Thymoquinone (TQ) have indicated remarkable effects on targeting multiple pathways potentially leading to apoptosis. The aim of the study augmenting the effects of TQ in overcoming cisplatin (CDDP) induced drug resistance in SKOV-3 cells.

Methods: The cells were treated with increasing doses of TQ in a time-dependent manner. The apoptotic bodies were analyzed by DAPI while the mitochondrial membrane potential was analyzed by Rh-123. The clonogenic assay was carried out to understand the colony formation potential. The protein expression for Bcl-2 and p53 were assessed using western blotting.

Results: The ability of TQ to overcome CDDP-induced drug resistance with the help of TQ in SKOV-3 cell lines. The minimum inhibition for SKOV-3 was 3 μ M for CDDP and 14 μ M for TQ. For the resistant SKOV-3, the minimum inhibition was 6 μ M for CDDP and 14 μ M for TQ. The apoptotic bodies, mitochondrial membrane, nuclear condensation, and nuclear fragmentation were the observed morphological changes. The colony formation assay revealed reducing in the formation of clones. The protein expressions displayed modifications in the levels of p53 and Bcl-2 in both cell lines.

Conclusion: TQ enhances apoptosis in SKOV-3 cells and is effective against the cells resistant to CDDP. This indicates a major application of TQ in recurrent OvCa that are resistant to CDDP.

Keywords: Ovarian cancer, thymoquinone, cisplatin, SKOV-3, cisplatin-resistance, apoptosis

¹ M.Sc PhD Scholar, Dr. Prabhakar Kore Basic Science Research Centre, KLE Academy of Higher Education and Research, Belagavi, India. - ORCID ID: <https://orcid.org/0000-0002-3936-6873>

² M.Sc, Maratha Mandal's Central Research Laboratory NGH, Bauxite Road, Belagavi, India. ORCID ID: <https://orcid.org/0000-0003-0533-0350>

³ M.Sc PhD, Dr. Prabhakar Kore Basic Science Research Centre, KLE Academy of Higher Education and Research, Belagavi, India. ORCID ID: <https://orcid.org/0000-0001-6261-1665>

⁴ M.Sc Maratha Mandal's Central Research Laboratory NGH, Bauxite Road, Belagavi, India. ORCID ID: <https://orcid.org/0000-0002-9861-4160>

⁵ MDS, Department of Public Health Dentistry, KLE VK Institute of Dental Sciences, KLE Academy of Higher Education and Research, Belagavi, India. ORCID ID: <https://orcid.org/0000-0003-3291-8716>

⁶ MD, PhD, Maratha Mandal's Central Research Laboratory NGH, Bauxite Road, Belagavi, India.

^{7*} M.Sc, PhD Dr. Prabhakar Kore Basic Science Research Centre, KLE Academy of Higher Education and Research, Belagavi, India. ORCID ID: <https://orcid.org/0000-0002-7463-8037>

***Corresponding Author:** Suneel Dodamani

*Basic Science Research Centre, KLE Academy of Higher Education and Research, Belagavi 590010, India, Contact number: +919901943638, E-mail ID: suneelddmn18@gmail.com

DOI: - 10.48047/ecb/2023.12.si5a.0337

INTRODUCTION

One of the primary causes of mortality worldwide is cancer, estimating 18.1 million deaths and 9.6 million new cases. OvCa is the second most common and lethal gynecological malignancy, often diagnosed at progressive stages. Signs and symptoms generally occur at advanced stages such as III and IV (1). There are different types of reported OvCa, with epithelial OvCa being the most prevalent one with a poor prognosis (2). The symptoms and signs of OvCa are indistinct, unclear, and vague. The risk factors include age, menstrual period, hormonal and infertility treatment, family history, genetic mutations, obesity, and socioeconomic status (3). After a sequence of platinum-based treatment or radiation, the majority of women experience a relapse of tumour or resistance to the drug and hence it is essential to develop innovative therapeutic approaches (4).

The recurrence of tumour can be associated with various factors such as DNA influx/efflux, drug target alteration, gene mutations, autophagy, epithelium-to-mesenchyme transition, tumour microenvironment, hypoxia, multi-drug resistance, DNA repair activation and cancer-associated fibroblasts (5). Various proteins involved in pathways like the PI3K pathway promote apoptosis in CDDP-sensitive cells that regulate proteins like Bcl-2 and Bax (6). These proteins may be modulated in the resistant cells and may not respond to CDDP. We study a similar mechanism in this investigation, as we compare the expression levels of these proteins in the SKOV-3 cells before and after inducing CDDP resistance. We induced resistance in the cell lines after repeated exposure to increasing concentrations of CDDP, which was confirmed by the cytotoxic assay, and further by comparing the apoptotic activities in resistant cells with the CDDP-sensitive ones.

The antiproliferative properties of TQ weaken the immune system while protecting the human body from other susceptible diseases. It provides oxidative damage in the cancer cells and maintains the homeostasis of normal cells. It reduces the expression of Bcl-2 (anti-apoptotic) on the hand and increases pro-apoptotic Bax expressions. It decreases the permeability of the mitochondrial membrane, triggers ROS, and activates other pro-apoptotic signaling pathways (7). TQ has shown synergistic effects in cancer cells by augmenting the cytotoxicity induced by cisplatin (8), through the regulation of Bax and Bcl-2 (9). Moreover, TQ has shown sensitizing activity in resistant cells

(10). In this study, TQ upregulated the pro-apoptotic proteins in the CDDP-resistant cells as seen by western blotting. In general, the efficacy of TQ was seen in resistant cells as compared to the CDDP-sensitive cells through the various assays in the study. The effect of TQ in CDDP-resistant SKOV-3 (R_SKOV-3) has not been reported, to the best of our knowledge and therefore, we attempt to investigate the same.

EXPERIMENTAL

Methods & Materials

Chemicals and reagents

Cisplatin and Thymoquinone (Sigma Aldrich), Dulbecco's Modified Eagle Medium (DMEM) (Gibco, Cat. No.-11965092), Antibiotic – Antimycotic (100X) solution (ThermoFisher Scientific, Cat. No.-15240062), and Fetal bovine serum (FBS) (Gibco, Cat. No.-10270106), MTT (3-(4,5-dimethylthiazol-2-yl)-2,5-diphenyltetrazolium bromide (Sigma Aldrich), DAPI (4',6-diamidino-2-phenylindole) (D9542). The apoptotic kit was Annexin V-FITC Apoptosis Detection Kit (R&D Systems, Cat. No. –4830-01-K). Propidium iodide (PI) (Cat. No.- P1304MP) was procured from ThermoFisher Scientific. The primary antibodies anti-beta, B-cell leukaemia (Bcl-2), and p53 were purchased from Jupiter Life Sciences. The secondary antibody IgG-HRP was procured from MERCK. Tetramethylbenzidine (TMB) (Cat. No.- T0565) was purchased from Sigma Aldrich. Dimethyl sulfoxide (DMSO) and paraformaldehyde were procured from Qualigens, India. For protein isolation, RIPA lysis buffer (Cat.no. TCL131) and protease inhibitor cocktail (ML051) were purchased from HiMedia.

Methods

Cell Culture

The SKOV-3 (human ovarian adenocarcinoma) cell line was obtained from National Center for Cell Science, Pune (India). SKOV-3 was cultured in McCoy's 5A (Modified) medium with 10% of FBS and 1% of the antibiotic-antimycotic solution. The cells were stored in a 5% CO₂ incubator at 37°C (New Brunswick Galaxy 170R, Eppendorf India Private Ltd., India). The cells were sub-cultured only after reaching 80% confluence for every experiment.

Cell viability assay

The cells were in the culture medium and grown until 80% confluency was achieved. Cells were then washed with PBS, detached using trypsin-EDTA, and counted using a hemocytometer. Further, 1X10² cells were seeded in a 96-well for

24h. These cells were incubated with different concentrations of CDDP and TQ for 24 and 48. The cells were suspended in 100µl of MTT solution for 3h and incubated at 37°C. The formazan crystals were dissolved in 100µl of DMSO. The optical density (OD) was measured using Lisa plus Microtitre Reader at 490nm. Untreated cells were used as control. All the groups were compared with the control group to calculate the percentage of cell viability. The inhibition concentration (IC₅₀) was analyzed for a dose-response study that involves 50% cell death for each drug. The statistical analysis was measured by the GraphPad Prism 5.1 software.

Formula: $Surviving\ cells\ (\%) = \frac{Mean\ OD\ of\ sample}{Mean\ OD\ of\ Negative\ control} \times 100$

CDDP resistance development

The parental cell lines were plated 1X10⁶ and incubated at 37°C stored at 5% CO₂ for 24h. The parental cells were treated with increasing concentrations of CDDP (starting from 0.2 µM) until the concentration was higher than the IC₅₀ value (3 µM) over a period of several days. The method used for the development of resistant cell lines was adapted from (11) with slight modifications.

Mitochondrial membrane potential (MMP)

The cells were grown in 24-well plates containing coverslips. On a subsequent day, the cells were treated with CDDP and TQ. The cells were washed with PBS 2-3 times after 48h. The cells were then stained with Rhodamine-123 (Rh-123) dye for 30 min. Further, the cells were washed with PBS and fixed using 4% PFA for 30mins. The cells were then examined under the fluorescent microscope and the intensity was calculated using GraphPad Prism 5.1.

Colony formation assay

The cells were seeded with a cell density of 1X10⁴ in 6cms plates at 37°C in 5% CO₂ overnight. After attachment, the cells were treated with 3 µM CDDP and 14 µM TQ for SKOV-3, and 14 µM of TQ for R_SKOV-3 according to the minimal inhibition concentration. After every 2 days, the culture medium was replaced for the cells to grow and incubated for 14 days at 37°C. After 14 days, the cells were washed with PBS 3 times and fixed with 4% PFA for 15min at room temperature. The colonies were stained with 0.4% crystal violet for 15min and further dried and counted. Each independent experiment was carried out in the same protocol for both SKOV-3 and resistant

SKOV-3. The statistical analysis was carried out using GraphPad Prism 5.1 software. The number of surviving colonies by the number of cells plated was used to calculate plating efficiency (PE). The cell survival fraction (SF) was the number of colonies that arise after treatment in terms of PE.

Formula: $SF\ (treated\ cells) = \frac{PE\ (treated\ cells)}{PE\ (control)}$

DAPI staining

The cells were seeded in a 24-well plate with coverslips and treated with CDDP and TQ after attachment. The cells were washed with PBS after 48h and fixed using 4% PFA for 30 min. 1µg/ml of DAPI was used to stain the cells incubated at RT in the dark for 5min. The cells were observed under the fluorescence microscope with 20X magnification and visualized using Pro RES® Capture Pro software (Jena, Germany).

Protein isolation

Cells were plated at 1X10⁶ density and then treated with CDDP and TQ for 48h. The cells were lysed using 500µl RIPA lysis buffer with 10µl of protease inhibitor for 1hr on ice with periodic vortexing. Further, the cells were transferred to 1.5 ml Eppendorf tubes and centrifuged at 12,000 rpm for 20mins (Eppendorf centrifuge 5810 R). The supernatant was collected in a new tube and stored at -4°C for further use (12).

Western blotting analysis

The isolated proteins were thawed and denatured at 100°C for 3min in a water bath. The proteins were separated by 7.5% sodium dodecyl sulfate-polyacrylamide gel (SDS-PAGE) for 2 ½h at 110V. The proteins from the gel were transferred onto a nitrocellulose membrane using a Towbin buffer containing 25 mM Tris, 192 mM glycine, pH 8.3 with 20% methanol (v/v) in a transfer chamber for 3h at 110V. After transfer the blot was blocked using 1% Bovine Serum Albumin overnight at 4 °C. The blot was washed with PBS thrice, 10 min each. The blot was treated with primary antibodies with 1% bovine serum albumin (BSA) overnight at 4°C. The primary antibodies used were anti-beta, B-cell leukemia (Bcl-2), and p53. The blot was washed with PBS thrice, 10 min each. Further, the blot was incubated using goat anti-mouse IgG-HRP with agitation for 3 h at room temperature. To view the bands, the blot was incubated in a TMB substrate for ½h. Rinse the blot with Milli Q water to stop the reaction.

Statistical analysis

All the above experiments were carried out in triplicates. The data was characterized as mean \pm standard deviation for each experiment. The groups were evaluated using a student's t-test for both treatment and control. The significance was established at a probability value ≤ 0.05 .

RESULTS & DISCUSSION

TQ stimulates anti-proliferative effects in SKOV-3 and resistant SKOV-3 cells

This study aimed to determine the effects of CDDP and TQ in SKOV-3 and R_SKOV-3 cells by adapting the procedures described by Almosa et al. (13). MTT assay was carried out in a time and concentration-dependent manner in SKOV-3 and R_SKOV-3 cells (Fig. 1). The IC₅₀ values for CDDP were found to be 2 μ M and 3 μ M for 24 h and 48h, respectively. The same was observed for TQ at 16 μ M and 14 μ M. The IC₅₀ values for 48h were used for further experiments. The SKOV-3 cells were subjected to the development of CDDP resistance by exposing them to increasing concentrations (Fig. 2). Minor morphological changes were observed over the course of this exposure. The IC₅₀ value of CDDP after the development of resistance was observed at 6 μ M while TQ at 14 μ M, was efficient to inhibit 50% of R_SKOV-3 cells. All the further assays were carried out in both SKOV-3 and R_SKOV-3 cell lines to assess the efficiency of the apoptotic activities of the compounds.

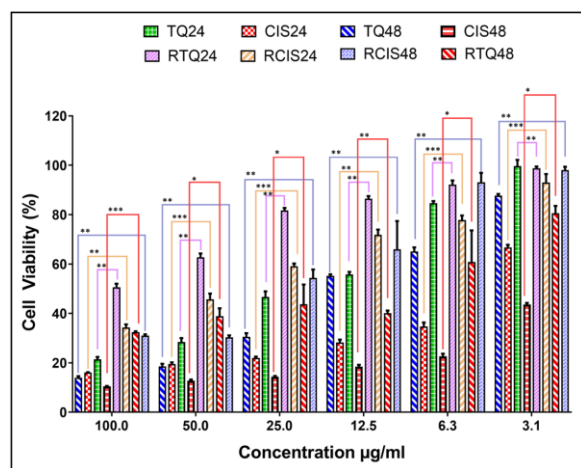


Fig. 1: Cytotoxicity in SKOV-3 after treatment with different concentrations of CDDP and TQ treatment for 24 and 48h.

(TQ24 = Treatment of SKOV-3 cells with TQ for 24h; CIS24 = Treatment of SKOV-3 cells with CDDP for 24h; TQ48 = Treatment of SKOV-3 cells with TQ for 48h; CIS48 = Treatment of SKOV-3 cells with CDDP for 48h; RTQ24 = Treatment of CDDP-resistant-SKOV-3 cells with TQ for 24h; RCIS24 = Treatment of CDDP-resistant-SKOV-3 cells with CDDP for 24h; RTQ48 = Treatment of CDDP-resistant-SKOV-3 cells with TQ for 48h; RCIS48 = Treatment of CDDP-resistant-SKOV-3 cells with CDDP for 48h)

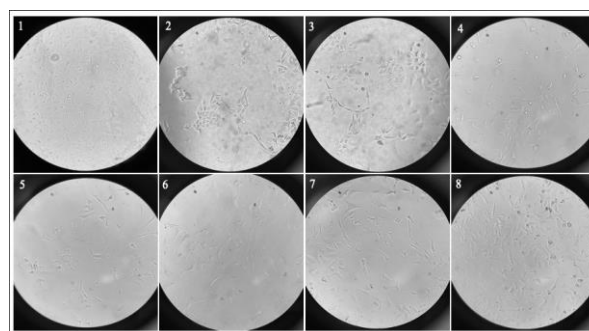


Fig. 2: Induction of CDDP resistance in SKOV-3 cell lines. The images indicate (1) SKOV-3 treated with 0.4 μ M/mL (2) SKOV-3 treated with 1.2 μ M/mL (3) SKOV-3 treated with 1.6 μ M/mL (4) SKOV-3 treated with 2 μ M/mL (5) SKOV-3 treated with 4 μ M/mL (6) SKOV-3 treated with 6 μ M/mL (7) SKOV-3 treated with 8 μ M/mL and (8) SKOV-3 treated with 10 μ M/mL.

TQ causes the mitochondrial dysfunction

The initiation of apoptosis consists of several biochemical changes, one of them being mitochondrial dysfunction. A change in the mitochondrial membrane potential (MMP) ($\Delta\Psi_m$) leads to membrane damage and the release of cytochrome c thereby causing apoptosis (14).

The $\Delta\Psi_m$ loss will be evaluated by using Rh-123 dye under a fluorescent microscope. The $\Delta\Psi_m$ loss is visualized by using Rh-123 dye under a fluorescent microscope. The mitochondrial dysfunction and organelle expansions are indicated by the leakage of dye. Upon treatment, SKOV-3 cells showed significant changes in the MMP, with TQ inducing maximum depolarization. In R_SKOV-3 cells, the CDDP treatment did not induce as much depolarization; while TQ was still effective (Fig. 3) (15).

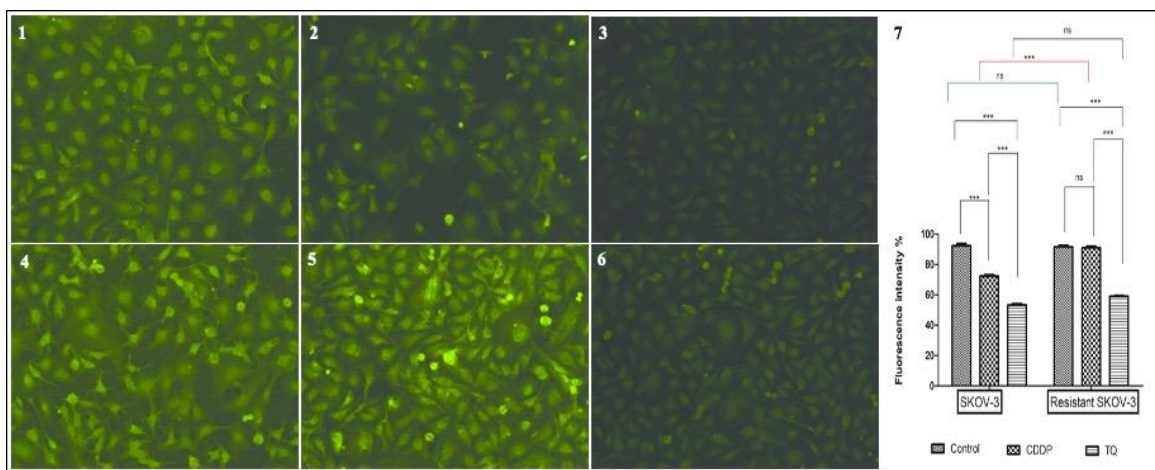


Fig. 3: MMP evaluation in SKOV-3 and R_SKOV-3. The images represent: (1) SKOV-3 untreated used as control (2) SKOV-3 treated with 3 $\mu\text{M}/\text{mL}$ of CDDP (3) SKOV-3 treated with 14 $\mu\text{M}/\text{mL}$ of TQ (4) R_SKOV-3 untreated (5) R_SKOV-3 treated with 6 $\mu\text{M}/\text{mL}$ of CDDP (6) R_SKOV-3 treated with 14 $\mu\text{M}/\text{mL}$ of TQ (7) The bar graph shows the fluorescent percentage in the above-stated groups. Data are expressed as mean \pm S.D. The significant difference is indicated as *** $p < 0.0001$, ** $p < 0.01$, and * $p < 0.05$ between control cells vs treated.

Morphological changes stimulated by TQ

The characteristics of early apoptosis are the nuclear and morphological modifications in cells. DAPI is a blue fluorescent dye that binds to DNA minor grooves. DAPI binds to both living and dead cells which can distinguish between the morphological transformations. The untreated cells show no or very little (due to natural cell death) morphological changes (16). The alterations in the morphology after treatment with a selected dose of

TQ for both SKOV-3 and R_SKOV-3 were observed by DAPI staining. After treatment with CDDP and TQ, nuclear condensation and fragmentation, blebbing membrane, and apoptotic bodies were observed. **Fig. 4** indicates the changes in the nuclear material further implying apoptosis via TQ treatment even in R_SKOV-3 when CDDP showed a diminutive response.

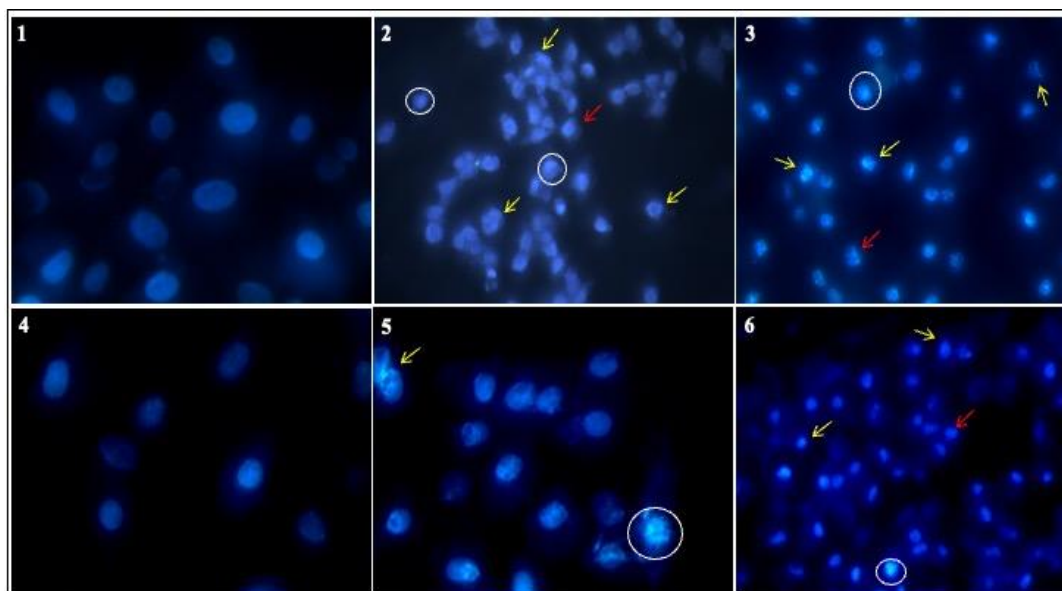


Fig. 4: Representation of fluorescent images after DAPI staining. The images describe: (1) The intact nuclei and high fluorescence intensity are shown in untreated SKOV-3 cells. (2) SKOV-3 treated with 3 $\mu\text{M}/\text{mL}$ of CDDP (3) SKOV-3 treated 14 $\mu\text{M}/\text{mL}$ of TQ (4) Untreated R_SKOV-3 (5) R_SKOV-3 treated with 6 $\mu\text{M}/\text{mL}$ CDDP (6) R_SKOV-3 treated with 14 $\mu\text{M}/\text{mL}$ of TQ. The images indicate nuclear membrane blebbing and apoptotic body formation (white circles), nuclear condensation (red arrows), and nuclear fragmentation (yellow arrows).

Effectiveness of TQ to form colonies post-treatment

The response to drug treatment in clonogenic cell survival indicates the efficacy of the drug (17). The survival of cancer cells in the presence of the drug, and their ability to form clones from a single cell characterizes the uncontrolled growth of cancer

(18). The results indicate that TQ significantly declines colony formation in both groups of cells, while multiple colonies continued to grow in the presence of CDDP, in the R_SKOV-3 cells (**Fig. 5**).

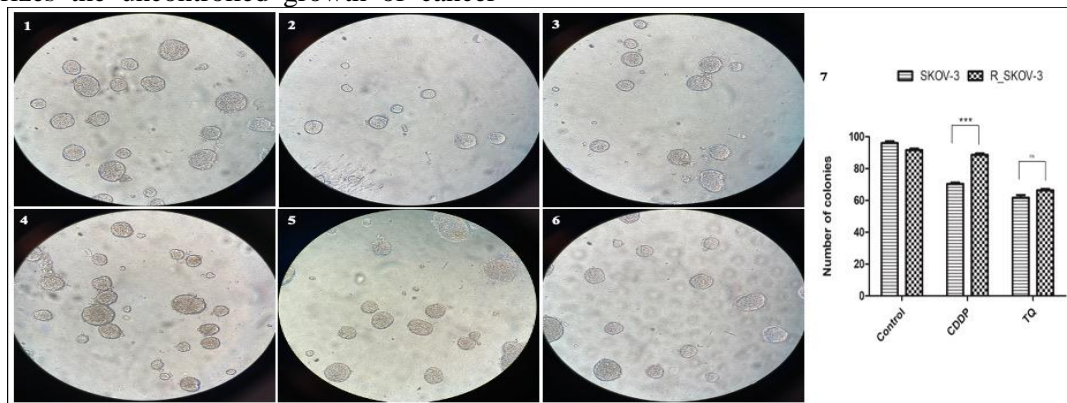


Fig. 5: SKOV-3 cells representing the colony formation assay after exposure to TQ and CDDP for 14 days. The images signify (1) Untreated SKOV-3 as control (2) SKOV-3 treated with 3 $\mu\text{M}/\text{mL}$ CDDP (3) SKOV-3 treated with 14 $\mu\text{M}/\text{mL}$ TQ (4) R_SKOV-3 untreated (5) R_SKOV-3 treated with 6 $\mu\text{M}/\text{mL}$ CDDP (6) R_SKOV-3 treated with 14 $\mu\text{M}/\text{mL}$ TQ. (7) Illustration of colony growth in CDDP and TQ.

The colonies were counted and the graph was plotted against untreated control for both. The bar graph represents data expressed as mean \pm S.D. The significance difference indicated as *** $p < 0.0001$, ** $p < 0.01$, and * $p < 0.05$.

TQ contributes to the modulation in the protein expressions

The modifications in the protein expression were analyzed for both SKOV-3 and R_SKOV-3 cells post-treatment with CDDP and TQ. Bcl-2 is an anti-apoptotic protein, activated in various cancers and closely related to chemoresistance, specifically studied in OvCa. The up-regulation of Bcl-2 instigates pro-survival activity in OvCa adding to tumorigenesis (19). Our results revealed that after the treatment with TQ and CDDP in SKOV-3, the

Bcl-2 expression significantly changed when compared to the control indicating their pro-apoptotic effects (**Fig. 6**). Alternatively in R_SKOV-3, Bcl-2 significantly reduced after TQ treatment. Secondly, p53 functions as a tumor-suppressor which is down-regulated in the cancer micro-environment enabling tumor progression. The gene responsible for p53 is also found to be mutated in cancers, which enables drug resistance (20). In SKOV-3, we observed a slight up regulation of p53 upon CDDP and TQ treatment. In R_SKOV-3 significant increase was observed in response to TQ, which was minimal in CDDP and control cells. This shows the regulation of apoptotic proteins by TQ in OvCa cells and its efficacy in its resistant counterpart.

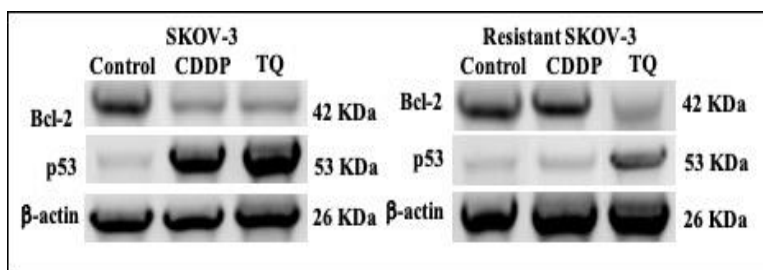


Fig. 6: Western blot analysis for p53 and Bcl-2 and the loading control was β -actin. (1) Representation of changes in protein expression of Bcl-2 and p53 for SKOV-3. (2) Representation of changes in protein expression of Bcl-2 and p53 for R_SKOV-3.

CONCLUSION

Naturally occurring compounds tend to synergically work with multiple pathways and

reduce toxicity levels while increasing the quality of life in patients. TQ has been demonstrated as a promising therapeutic agent to overcome drug resistance and alleviate adverse effects. It has

cytoprotective roles on drugs like CDDP, carboplatin, paclitaxel, cyclophosphamide, etc., which prove its potential forthcoming clinical uses. Its effects make individuals less susceptible to other diseases in turn protecting them from the weakening of the immune system. Also, it shields normal human cells from oxidative damage while decreasing mitochondrial permeability, dropping Bcl-2, and enhancing Bax expression in cancer. It produces excessive ROS, and DNA damage, activating signaling pathways and further causing apoptosis of cancer cells. It also helps to overcome drug resistance by obstructive the progression of cells. TQ can be used as broadly used as a novel therapeutic in the treatment of OvCa and several other types. Hence, TQ proves to be a suitable candidate to be taken up to clinical trials to remarkably combat distinctive types of cancer.

Statement and Declarations

Funding: No funding was involved in the project

Conflict of Interest

The authors declare no competing interests.

Author Contributions

All the authors contributed to the study design. Material preparation, data collection, and analysis were performed by Shivani Tendulkar and Aishwarya Hattiholi. Dr Vijay Kumbar helped with data analysis. Ms Meenaz Sangolli helped with the protein analysis. Dr Suneel Dodamani, Dr Kishore Bhat and Dr Mehul Shah commented on previous versions of the manuscript. All authors read and approved the manuscript.

REFERENCES

1. Bray F, Ferlay J, Soerjomataram I. Global Cancer Statistics 2018: GLOBOCAN Estimates of Incidence and Mortality Worldwide for 36 Cancers in 185 Countries. *A Cancer Journal for Clinicians*. 2018;68(4):394–424.
2. Stewart C, Ralyea C, Lockwood S. Ovarian Cancer: An Integrated Review. *Semin Oncol Nurs* [Internet]. 2019;35(2):151–6. Available from: <https://doi.org/10.1016/j.soncn.2019.02.001>
3. Momenimovahed Z, Tiznobaik A, Taheri S, Salehiniya H. Ovarian cancer in the world: epidemiology and risk factors. *Int J Womens Health*. 2019;11:287–99.
4. Kumar S, Kushwaha PP, Gupta S. Emerging targets in cancer drug resistance. *Cancer Drug Resistance*. 2019;2:161–77.
5. Zhou J, Kang Y, Chen L, Wang H, Liu J, Zeng S, et al. The Drug-Resistance Mechanisms of Five Platinum-Based Antitumor Agents. *Front Pharmacol*. 2020;11(March):1–17.
6. Stewart JJ, White JT, Yan X, Collins S, Drescher CW, Urban ND, et al. Proteins associated with cisplatin resistance in ovarian cancer cells identified by quantitative proteomic technology and integrated with mRNA expression levels. *Molecular and Cellular Proteomics*. 2006;5(3):433–43.
7. Imran M, Rauf A, Khan IA, Shahbaz M, Qaisrani TB, Fatmawati S, et al. Thymoquinone: A novel strategy to combat cancer: A review. Vol. 106, *Biomedicine and Pharmacotherapy*. Elsevier Masson SAS; 2018. p. 390–402.
8. Wilson AJ, Saskowski J, Barham W, Yull F, Khabele D. Thymoquinone enhances cisplatin-response through direct tumor effects in a syngeneic mouse model of ovarian cancer. *J Ovarian Res*. 2015 Jul 28;8(1).
9. Liu X, Dong J, Cai W, Pan Y, Li R, Li B. The effect of thymoquinone on apoptosis of SK-OV-3 ovarian cancer cell by regulation of Bcl-2 and Bax. *International Journal of Gynecological Cancer*. 2017;27(8):1596–601.
10. Nessa Meher, PHILIP BEALE, CHARLES CHAN, JUN Q. YU and, FAZLUL HUQ1. Synergism from Combinations of Cisplatin and Oxaliplatin with Quercetin and Thymoquinone in Human Ovarian Tumour Models. *Anticancer Res*. 2011;31:3789–98.
11. Govindan SV aliyaveedan, Kulsum S, Pandian RS omasundara, Das D, Seshadri M, Hicks W, et al. Establishment and characterization of triple drug-resistant head and neck squamous cell carcinoma cell lines. *Mol Med Rep*. 2015 Aug 1;12(2):3025–32.
12. Kirby ED, Kuwahara AA, Messer RL, Wyss-Coray T. Adult hippocampal neural stem and progenitor cells regulate the neurogenic niche by secreting VEGF. *Proc Natl Acad Sci U S A*. 2015 Mar 31;112(13):4128–33.
13. Almosa H, Alqriqi M, Denetiu I, Baghdadi MA, Alkhaled M, Alhosin M, et al. Cytotoxicity of standardized curcuminoids mixture against epithelial ovarian cancer cell line SKOV-3. *Sci Pharm*. 2020 Mar 1;88(1).
14. Zorova LD, Demchenko EA, Korshunova GA, Tashlitsky VN, Zorov SD, Andrianova N v., et al. Is the mitochondrial membrane potential ($\Delta\Psi$) correctly assessed? intracellular and intramitochondrial modifications of the $\Delta\Psi$ probe, rhodamine 123. *Int J Mol Sci*. 2022 Jan 1;23(1).
15. Hattiholi A, Tendulkar S, Kumbar V, Rao M, Kugaji M, Muddapur U, et al. Evaluation of

- Anti-cancer Activities of Cranberries Juice Concentrate in Osteosarcoma Cell Lines (MG-63). *Indian Journal of Pharmaceutical Education and Research*. 2022 Oct 1;56(4):1141–9.
16. Rahman MA, Hussain A. Anticancer activity and apoptosis inducing effect of methanolic extract of *Cordia dichotoma* against human cancer cell line. *Bangladesh J Pharmacol*. 2015;10(1):27–34.
17. Bendale Y, Bendale V, Paul S. Evaluation of cytotoxic activity of platinum nanoparticles against normal and cancer cells and its anticancer potential through induction of apoptosis. *Integr Med Res*. 2017 Jun;6(2):141–8.
18. Matsui T, Nuryadi E, Komatsu S, Hirota Y, Shibata A, Oike T, et al. Robustness of clonogenic assays as a biomarker for cancer cell radiosensitivity. Vol. 20, *International Journal of Molecular Sciences*. MDPI AG; 2019.
19. Yuan J, Lan H, Jiang X, Zeng D, Xiao S. Bcl-2 family: Novel insight into individualized therapy for ovarian cancer (Review). Vol. 46, *International Journal of Molecular Medicine*. Spandidos Publications; 2020. p. 1255–65.
20. Zhang Y, Cao L, Nguyen D, Lu H. TP53 mutations in epithelial ovarian cancer. Vol. 5, *Translational Cancer Research*. AME Publishing Company; 2016. p. 650–63.